EurJOC
European Journal of Organic Chemistry

Research Article
doi.org/10.1002/ejoc.202101436

Chemistry Europe
European Chemical Societies Publishing

www.eurjoc.org

Regioselective Hydroxylation of Stilbenes by White-Rot Fungal P450s Enables Preparative-Scale Synthesis of Stilbenoids

Nico D. Fessner,*[a] Hansjörg Weber,[b] and Anton Glieder[a]

Scaling up biocatalytic reactions involving cytochrome P450 monooxygenases (P450s) is challenging due to their instability, low substrate loading, co-factor, and oxygen requirements as well as the dependency on a reductase partner, which limits their integration into synthetic chemistry. Recently, a biocatalytic study investigated frequently used bacterial P450s to produce bioactive stilbenoids, extending the repertoire of sustainable synthetic strategies with remarkable success. This article explores the complementary application of less common eukaryotic P450s as a viable alternative for generating the same compounds when employed as a *Pichia pastoris*-based whole-cell biocatalyst. In a direct comparison to their bacterial equivalents, the recently discovered P450s CYP5035S7 and CYP5035S9 from the white-rot fungus *Polyporus arcularius* are shown to be competitively efficient at synthesising stilbenoids at preparative-scale.

Introduction

Stilbenoids are bioactive natural products acting as a two-edged sword. As plant phytoalexins, they are produced to protect the host by exhibiting a lethal impact on pathogens and fungi.[1,2] For humans, however, stilbenoids are interesting due to all kinds of pharmaceutically relevant properties.[3,4] (*E*)-resveratrol is a prominent example that is advertised for encompassing many health-related beneficial properties,[5,6] and also the related stilbenoid (*E*)-4,4′-dihydroxystilbene raised attention with its enhanced anti-tumour properties.[7,8]

The extraction of these substances from natural sources is low-yielding, costly and unsustainable.[9] To cover the supply of these stibenoids, metabolic engineering is probably most promising, as evidenced by excellent studies in the past few years reporting titres of up to 800 mg/L.[10,11]

In addition, there is a large portfolio of strategies for the synthesis of functionalised stilbenes available, which range from simple aldol-type condensations to palladium-catalysed coupling reactions and were extensively reviewed in the past.[12–14] However, oftentimes these chemical reactions involve multiple steps, toxic reagents, high energy consumption and unsustainable transition metal catalysts. They may also lack high yields or high selectivity, contaminating products and disregarding them for the use as medicines.

In contrast, biocatalysis operates under mild conditions and is considered as environmentally friendly and sustainable. In addition, cytochrome P450 monooxygenases (P450s) possess the ability to target unactivated C–H bonds in a synthetic late-stage fashion and in the presence of reactive functional groups. Ultimately, readily available (*E*)-stilbene can be used as the starting material,[15] which is only hydroxyl groups short to the desired stilbenoid product structures. Therefore, two studies investigated oxyfunctionalisation enzymes for the production of stilbenoid analogues[16,17] as alternatives to other green methods.[18] Urlacher *et al.*[17] synthesised stilbenoids on a preparative scale using engineered bacterial P450s, which proved very effective for regioselective late-stage hydroxylation of natural products.[19] Efficient reactivity of the bacterial P450 was eventually achieved after several rounds of active-site protein engineering. Albeit executed at very small scale, one year later Gutiérrez *et al.*[16] demonstrated that the up-coming unspecific peroxygenases (UPOs) with similar reactivity to P450s,[20] can be used for the same purpose.

As compared to their soluble and self-sufficient bacterial counterparts, membrane-bound eukaryotic P450s require the co-expression of a suitable reductase partner for efficient electron transfer from the NAD(P)H co-factor.[21] This makes eukaryotic P450s generally less attractive for synthetic application, although remarkable successes were already achieved for example with human[22–24] or fungal P450s.[25–28] Sequence truncation to eliminate their membrane-anchor can impair stability significantly,[29] which is why they are usually used as heterologous biocatalysts in form of whole-cells, which provide a natural cellular environment for these eukaryotic enzymes.[30,31] P450s can be used as homogeneous catalysts for the synthesis of useful product quantities, efficiently in

[a] *Dr. N. D. Fessner, Prof. Dr. A. Glieder*
Institute of Molecular Biotechnology
Graz University of Technology
Petersgasse 14, 8010 Graz, Austria
E-mail: nico.fessner11@alumni.imperial.ac.uk
[b] *Prof. Dr. H. Weber*
Institute of Organic Chemistry
Graz University of Technology
Stremayrgasse 9, 8010 Graz, Austria

Supporting information for this article is available on the WWW under https://doi.org/10.1002/ejoc.202101436

Research Article
doi.org/10.1002/ejoc.202101436

particular when applying self-sufficient P450s. Generally though, heterogeneous whole-cell application is preferred for P450 up-scaling experiments to account for biological characteristics such as co-factor dependence.[21,32–34]

White- and brown-rot fungal P450 monooxygenases are particularly intriguing because their native function includes the detoxification of plant xenobiotics to help maintain the fungus' wood-degrading lifestyle.[28,35] Therefore, stilbene phytoalexins were used as model substrates to characterise P450s of Basidiomycota and many P450s were found to not only accept stilbenoid phytoalexins as natural substrates, but also convert them very efficiently.[36,37] However, despite this known catalytic potential,[25–28] individual basidiomycete P450s had never been tested for the synthesis of stilbenoids in synthetically useful quantities.

Therefore, in this article we aimed at establishing such eukaryotic P450s as an alternative to already available bacterial enzymes for the preparative multi-mg-scale conversion of (*E*)-stilbene (**1**), forming (*E*)-4-hydroxystilbene (**2**) and (*E*)-4,4′-dihydroxystilbene (**3**), and (*E*)-pinosylvin (**4**), to yield (*E*)- (**5**) and (*Z*)-resveratrol (**6**) (Scheme 1). For this purpose, we used our two recently identified xenobiotic-detoxifying P450s, CYP5035S7 and CYP5035S9, of the white-rot fungus *Polyporus arcularius*, which had shown activity towards **1**.[36] The efficient expression of these two P450s in *Pichia pastoris* (*Komagataella phaffii*) co-expressed with the yeast's P450 reductase enabled such scale without the need for (i) the native fungal P450 reductase or (ii) directed evolution of the biocatalysts. Moreover, the application of whole-cell biocatalysts rendered the need for (iii) addition and regeneration of co-factor unnecessary.[34]

Results and Discussion

Both CYP5035S7 and CYP5035S9 were found to metabolise 1 mM of **1**,[36] each forming a slightly different product profile according to HPLC analysis (Figure 1). While the former P450 gave mainly rise to a single product peak at $R_f = 2.7$ min, a second peak was more dominantly present at $R_f = 3.4$ min for the latter monooxygenase. Without access to (commercial) authentic reference compounds, preparative isolation was necessary to resolve the product structures.

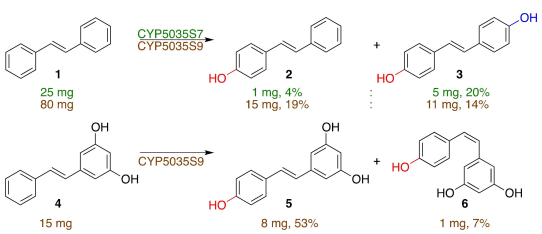

Scheme 1. (Consecutive) *para*-hydroxylation of compounds **1** and **4** catalysed on a preparative-scale by eukaryotic P450 enzymes CYP5035S7 and CYP5035S9 in *P. pastoris* whole-cells in this study.

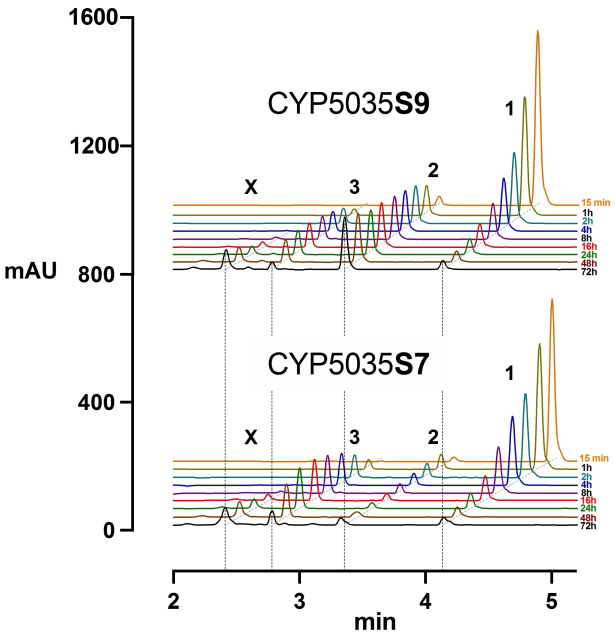

Figure 1. HPLC monitoring of the reaction progress of the bioconversion of **1** using CYP5035S9 and CYP5035S7 over the time course of 72 hours (1 mM of **1**, ca. 70 mL, OD600 = 200, 120 rpm, 72 h, 28 °C).

Firstly, different whole-cell biocatalyst quantities (optical density, $OD_{600} = 50$, 100, 200, 240; Figures S1 and S2) and different substrate concentrations (0.5, 1, 2, 5 mM; Figures S3–S6) were tested in order to elaborate the most favourable reaction conditions to be used for preparative-scale biotransformations. Even at an $OD_{600} = 200$ and 0.5 mM substrate concentration, complete substrate consumption could not be achieved with either P450. However, for both P450s, higher OD and lower substrate concentration led to an improved conversion as expected. Therefore, we decided to use an OD_{600} of 200 and 1 mM substrate concentration for subsequent preparative experiments because higher ODs would increase the required biomass to an impractical extent, and 1 mM substrate concentration compared to 0.5 mM produced a larger product quantity calculated by peak integration at still good conversion rate.

Next, we deduced an appropriate reaction time by following the reaction progress of the conversion of **1** by both CYP5035S7 and CYP5035S9 over the time course of 72 hours in an enlarged volume of 70 mL (Figure 1).

Thereby, the appearance of a third product peak at $R_f =$ 2.4 min was noticed during prolonged reaction time, increasing in intensity after about eight hours. Interestingly, the concentration of **3** declined during this period pointing towards a cell-induced decomposition of **3** to this side-product **X**. However, the peaks at the same elution time were later also noticed in the biotransformations of derivatives of **1** pointing towards a specific (metabolic) product intrinsically produced by *P. pastoris*, which was potentially induced by the biotransformation. Despite spectroscopic analysis, its structure could not be unambiguously resolved. As a consequence, the subsequent biotransformations of **1** were limited to 16 hours.

Research Article
doi.org/10.1002/ejoc.202101436

Finally, we executed preparative-scale biotransformations by using 2x (CYP5035S7) and 6x (CYP5035S9) shake flasks each containing ca. 70 mL of cell broth. The conversion of 25 and 80 mg of **1** was catalysed by CYP5035S7 (Figure S7) and CYP5035S9 (Figure S8), respectively, as the latter monooxygenase promised larger quantities of both compounds for structure analysis by NMR spectroscopy.

Indeed, 1 and 5 mg as well as 15 and 11 mg of products **2** and **3** were obtained when using CYP5035S7 or CYP5035S9, equalling overall yields of 24 and 33%, respectively. In each case, about 8 mg of substrate **1** was recovered, too. Both catalysts clearly hydroxylated the *para*-positions of **1** with high regioselectively, favoured by electron-activation combined with steric accessibility. These two features were already deduced as guiding factors of CYP5035S7's reactivity in our previous studies.[38,39]

Mass-transfer limitations are a known problem in the substrate diffusion across the cell membrane to the intracellular enzyme and adversely affect whole-cell biotransformations in terms of final product yield.[31,40] Clearly, the extent of this effect depends on the hydrophilicity of the substrate, which is poor in the case of **1**. Hence, the yields obtained here are clearly subject to improvement, for example by using biphasic biotransformations for more efficient mass-transfer.[41,42]

Detailed investigation of the functionality of such white-rot fungal P450s is scarce and predictions from sequence alone is challenging[43] considering that the percentage identity of P450s often differs significantly even among members of the same subfamily (>55% ID).[44] For example CYP5035S7 and CYP5035S9 align with 67.6% ID only. Therefore, we investigated the substrate scope of the two P450s towards (*E*)-stilbene-like compounds by screening them against a small library of structural analogues and derivatives (Figure 2), in order to obtain a clearer picture of the enzymes' reactivity and utility. Both variants showed an extended substrate tolerance. Smaller entities such as styrene (**7**) and (*E*)-β-methylstyrene (**8**) remained unconverted, indicating their molecular structures to be inappropriate for a stable and productive binding in the active pocket. However, related coumpounds such as (*Z*)-stilbene (**9**), (*E*)-1,2-diphenylacetylene (**10**) and (*E*)-α-methylstilbene (**11**), albeit with decreasing conversion. While **10** was converted just as fast as **1**, already a small substituent like the α-methyl group of **11** decreased the conversion rate by 3-fold. Hence, it seems obvious why the sterically demanding triphenylethylene (**12**) was not accepted. Apparently, the presence of an epoxide in (*E*)-stilbene oxide (**13**) was also detrimental, however, the lower electron-density of the aromatic rings are likely to be the reason for this observation. As expected, compound **2** was accepted as a substrate by both enzymes and converted to **3** as seen by the kinetic profile plotted in Figure S9. Intriguing was also the information that could be read off the biotransformation of **14** because the methoxy group meant the introduction of a new functional group. Despite the polar oxygen, the masking of the methyl group caused the elution time to **14** to be almost the same as that of **1**. Two peaks appeared in the same pattern as for **1**, however, only the more polar one aligned perfectly with the elution time of the product peak corresponding to **3** (Figure S10). Therefore, **14** was rapidly hydroxylated by CYP5035S7 at the unsubstituted 4'-position and slowly demethylated the 4-methoxy functional group to finally yield the dihydroxylated product **4**. The rates of CYP5035S9 to do the same were much lower, but a small peak for the demethylation product was also observed (Figure S11).

Notably, the formation of side-product **X** occurred in the biotransformation of each of the substrates indicating **X** to be rather of metabolic nature produced by the yeast cells – a phenomenon that we had experienced previously for different substrates.[22,38] The elution times of the main products of **9**–**11** and **14** suggested (at least) one mono- and one di-hydroxylated product each just as in the case of **1**, which makes the same *para*-hydroxylation selectivity likely (Figures S10 and S11). In case of **9**, product peaks eluted even at exactly the same time suggesting partial (*Z*)- to the more stable (*E*)-isomerisation caused by light exposure before enzymatic hydroxylation took place.

The most interesting result of Figure 2, however, really was the discrimination of **4** showing excellent conversion by CYP5035S9, but not CYP5035S7. This result was surprising given the latter's fast rate at hydroxylation of stilbenoid **2** to form **3** (Figure S9) and its characterisation as a promiscuous enzyme with a broad substrate scope as revealed by the previous comprehensive screening.[36] From the analytical-scale reaction catalysed by CYP5035S9 only a single product peak appeared, which was assigned to be the mono-hydroxylated compound **5** according to the a) matching elution times with authentic **5** and b) *para*-selective reaction pattern, which showed c) high similarity to that observed using the bacterial P450 in the aforementioned study by Urlacher *et al.*[17]

A preparative-scale conversion of 15 mg of **4** was executed for product confirmation (Figure S12). Although only a single product and no remaining substrate were observed by analytical HPLC, the ^{1}H NMR spectrum of the extracted material

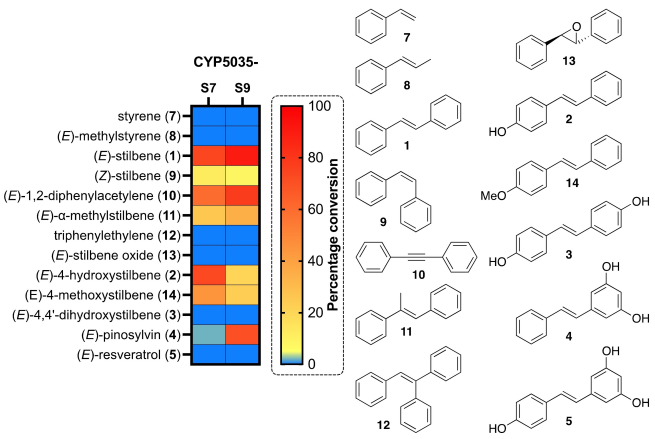

Figure 2. Stilbenoid substrate profiling: (*E*)-stilbene and various derivatives on the right (sorted by increasing structural complexity) were screened by CYP5035S7 and CYP5035S9 (1 mM, 400 µL, OD600 = 100, 320 rpm, 16 h, 28 °C). The heat map on the left indicates the conversion efficiency calculated by HPLC peak integration of newly appeared peaks.

Table 1. Comparison of the preparative-scale bioconversions of **4** by the bacterial P450 mutant CYP154E1QVA reported by Urlacher *et al.*[17] *versus* by the native white-rot fungal P450 CYP5035S9 employed in this study.

	Bacterial P450 (Urlacher *et al.*)[17]	**Eukaryotic P450** (this study)
Expression host	*Escherichia coli*	*P. pastoris*
Biocatalysis	Purified enzymes	Whole-cell BT[a]
P450 enzyme	CYP154E1 mutant QVA (*T. fusca*)[b]	CYP5035S9 (*P. arcularius*)
P450 reductase	YkuN (*B. subtilis*)[c] & FdR (*E. coli*)[d]	Host reductase co-expressed
Co-factor (addition & regeneration)	NADPH (200 μM), glucose, GDH (*B. megaterium*)[e]	–
Additives	Catalase (bovine liver)	–
Reaction vessel	Round-bottom flask	Shake-flask
Conditions	25 °C, magnetic stirring	28 °C, 120 rpm shaking
Reaction volume	10 mL	72 mL
P450 concentration	1 μM	$OD_{600} = 200$
Substrate **4**	1 mM (2.3 mg)	1 mM (15 mg)
Reaction time	20 h	16 h
Conversion (HPLC)	100 %	100 %
Isolated product **5** (+**6**)	1.9 mg	8 mg (+1 mg)
Yield of **5** (+**6**)	83 %	53 % (+7 %)
Efficiency of biocatalysis	TTN < 20,000	Productivity[f] = 0.32 %
Scalability	Purified proteins	Biomass & OD
Cost & time aspects	Cell lysis, protein purification, NADPH	Longer cultivations

[a] Biotransformation. [b] *Thermobifida fusca*. [c] flavodoxin of *Bacillus subtilis*. [d] flavodoxin reductase of *Escherichia coli*. [e] glucose dehydrogenase of *Bacillus megaterium*. [f] productivity[40] [g/g] = product weight/dry cell weight.

indicated a minor secondary product. After purification by preparative HPLC the major product (8 mg) could indeed be confirmed as **5**. The minor isolated product (1 mg), which migrated close to **5**, possessed a very similar ^{1}H NMR signal pattern except for a pronounced shift difference of the alkene-proton peaks and overall more shielded signals, and was therefore concluded to be (*Z*)-resveratrol. Either undesired light exposure had caused partial isomerisation to the thermodynamically less stable (*Z*)-isomer during the isolation procedure, or this was caused during the oxidation reaction by the P450. In total, an overall yield of 60 % was obtained upon 100 % conversion of 1 mM of **4** within 16 h. The higher yield achieved with the conversion of **4** compared to that of **1** might be due to the more hydrophilic nature of the substrate reducing the mass-transfer limitations discussed before.

As shown in Table 1, these percentages represent a similar conversion but somewhat lower yield (due to the whole-cell approach) at slightly shorter reaction time relative to the study of Urlacher *et al.* using the purified bacterial CYP154E1 mutant QVA.[17] In addition to protein engineering, the bacterial system was optimised using additives and a co-factor regeneration system, however, only a small volume and a low P450 concentration (1 μM) was required to obtain their reported yield.

In contrast, our endeavour did not involve any enzyme engineering (*cf.* CYP154E1),[17] optimisation of reaction conditions (*eg.* solubility of **4**)[40] nor *P. pastoris* colony/strain selection (due to possible gene loci effects on recombinant protein production)[45,46] in the case of CYP5035S9.[36] We also did not require the addition of expensive co-factor due to the whole-cell system providing it.

Moreover, no tedious protein purifications were required, decreasing the overall sample handling time and costs.[47,48] Instead, a strong bidirectional promoter[49] for the co-expression of *P. pastoris*' native P450 reductase,[36] the hydrophobic nature of the cell membrane[31,40] for good substrate uptake and the cellular co-factor recycling[34] make the presented preparative *P. pastoris* whole-cell biotransformation easily applicable and scalable. For example, up-scaling was executed simply by producing more biomass and adding 1 mM of substrate to the cell broth at selected OD. Simultaneously, for this reason biotransformations at analytical scale with different ODs may be recommended to further explore a possible intervention of other enzymes of the host cells' intrinsic metabolic enzymes.

Ultimately, the comparison in Table 1 showcases both the potential efficiency of eukaryotic, white-rot fungal P450 enzymes targeting their natural substrates in combination with stabilising cellular environment, but also a potential deficit of whole-cell biotransformations.

Conclusion

In conclusion, the two white-rot fungal P450s CYP5035S7 and CYP5035S9 metabolised **1** as well as structural analogues and stilbenoid derivatives efficiently and with high regioselectivity. This study illustrates that eukaryotic P450 enzymes can enable extraordinary bioconversions of natural products such as stilbenoids with competitive efficiency at preparative scale to bacterial P450s as demonstrated with the example of the CYP5035S9-catalysed conversion of **4**. Albeit reduced yields were identified as a key disadvantage of a whole-cell biotransformation, they are compensated by excellent enhancement of P450 stability, versatile co-factor supply and easy scalability using the biomass. Additionally, the remarkable partnership of *P. pastoris*' intrinsic P450 reductase with these two white-rot fungal P450 enzymes should be highlighted enabling the facile up-scaling to preparative amounts. All in all,

this study provides excellent prerequisites for further exploration of white-rot fungal P450 enzymes for synthetic purposes.

Experimental Section

Solvents and chemicals were purchased in best available purity and used as received without further purification from Sigma-Aldrich/Merck (Steinheim/Darmstadt, Germany), VWR International (Fontenay-sous-Bois, France), Carl Roth GmbH (Karlsruhe, Germany) or Fisher Scientific (Loughborough, UK). The *P. pastoris* strain expressing CYP5035S7 enzyme from a previous study was used.[36] HPLC tubes from Macherey-Nagel (Düren, Germany) and the corresponding caps and inserts from Bruckner Analysentechnik (Linz, Austria) were utilised. The Eppendorf BioPhotometer plus was used for OD measurements. A Bruker Avance III 300 MHz NMR spectrometer equipped with an autosampler recorded the NMR spectra or a Varian/Agilent Inova 500 MHz NMR spectrometer equipped with an indirect detection probe 5 mm. Agilent Technologies 1260 Infinity HPLC system coupled to a 6120 quadruple LC/MS mass detector (MSD) confirmed the mass of each isolated product.

Substrate screening: The same protocols and conditions described previously[36] were applied for protein expression using the *P. pastoris* strain expressing CYP5035S7 monooxygenase, for biotransformations to carry out the substrate screening (OD_{600} = 100, 0.4 mL, 1 mM, 17 h, 28 °C, 320 rpm) and for the HPLC analysis (280 nm), which employed the same HPLC instrument and column. The biotransformations were tested at different cell (OD_{600}: 50, 100, 200, 240; Figure S1 and S2) and substrate concentrations (0.5, 1, 2, 5 mM; Figure S3–S6).

Product isolation: Sufficient biomass for the preparative biotransformation was produced by strain cultivation in several baffled 2.5 L shake flasks (2x, 6x and 1x ca. 70 mL of biotransformation of **1** by CYP5035S7 and CYP5035S9, and of **4** by CYP5035S9, respectively). The same protocols, conditions and preparative HPLC purification method (but using 280 nm for product detection) as described previously[38,39] was applied for the product isolation. Hence, in total 25 mg (0.139 mmol) of **1** was added in case of the biotransformations catalysed by CYP5035S7 (Figure S7); 80 mg (0.443 mmol) of **1** (Figure S8) or 15 mg (0.071 mmol) of **4** (Figure S12) using CYP5035S9. The biotransformations were carried out for 16 hours at 28 °C, 80 % humidity and 120 rpm.

(*E*)-stilbene (**1**, $C_{14}H_{12}$, white solid, 9 mg (36 %) and 8 mg (10 %) using CYP5035S7 and CYP5035S9, respectively).

(*E*)-4-hydroxystilbene (**2**, $C_{14}H_{12}$, white-green solid, 1 mg (4 %) and 15 mg (19 %) using CYP5035S7 and CYP5035S9, respectively): ^{1}H NMR (300 MHz, Acetone-d_6): 8.50 (1H, br, 4-OH), 7.56 (2H, d, J = 8.0 Hz, 2′-, 6′-H), 7.47 (2H, d, J = 8.5 Hz, 2-, 6-H), 7.34 (2H, dd, J = 8.0, 7.5 Hz, 3′-, 5′-H), 7.22 (1H, dd, J = 7.5, 7.5 Hz, 4′-H), 7.15 (1H, d, J = 16.3 Hz, α′-H), 7.02 (1H, d, J = 16.3 Hz, α-H), 6.87 (2H, d, J = 8.5 Hz, 3-, 5-H). The HSQC spectrum provided ^{13}C shifts similar to literature.[50,51]

(*E*)-4,4′-dihydroxystilbene (**3**, $C_{14}H_{12}O_2$, yellow solid, 5 mg (20 %) and 11 mg (14 %) using CYP5035S7 and CYP5035S9, respectively): ^{1}H NMR (300 MHz, Acetone-d_6): 8.40 (2H, br, 4-, 4′-OH), 7.41 (4H, d, J = 8.5 Hz, 2-, 6-, 2′-, 6′-H), 6.96 (2H, s, α-, α′-H), 6.84 (4H, d, J = 8.5 Hz, 3-, 5-, 3′-, 5′-H). The HSQC spectrum provided ^{13}C shifts similar to literature.[52]

(*E*)-resveratrol (**5**, $C_{14}H_{12}O_3$, white crystals, 8 mg (53 %) using CYP5035S9): ^{1}H NMR (300 MHz, Acetone-d_6): 8.31 (3H, br, 3-, 5-, 4′-OH), 7.43 (2H, d, J = 8.5 Hz, 2′-, 6′-H), 7.05 (1H, d, J = 16.2 Hz, α′-H), 6.91 (1H, d, J = 16.2 Hz, α-H), 6.85 (2H, d, J = 8.5 Hz, 3′-, 5′-H), 6.54 (2H, d, J = 2.1 Hz, 2-, 6-H), 6.27 (1H, d, J = 2.4, 2.1 Hz, 4-H). The HSQC spectrum provided ^{13}C shifts. The NMR data was confirmed by comparison to that in the literature.[53–56]

(*Z*)-resveratrol (**6**, $C_{14}H_{12}O_3$, white crystals, 1 mg (7 %) using CYP5035S9): ^{1}H NMR (300 MHz, Acetone-d_6): 8.25 (3H, br, 3-, 5-, 4′-OH), 7.15 (2H, d, J = 8.5 Hz, 2′-, 6′-H), 6.71 (2H, d, J = 8.5 Hz, 3′-, 5′-H), 6.45 (1H, d, J = 12.3 Hz, α′-H), 6.34 (1H, d, J = 12.3 Hz, α-H), 6.28 (2H, d, J = 2.1 Hz, 2-, 6-H), 6.22 (1H, d, J = 2.1, 2.1 Hz, 4-H). The proton spectrum was an upfield-shifted version to that of **5** with an additional shielding effect of the alkene protons, strongly suggesting the identity of a (*Z*)-isomerism compared to the already identified (*E*)-isomerism. The deduced structure was confirmed by comparing to literature.[53,55]

Author contribution

N.D.F. devised the study concept and conducted all experiments. N.D.F. and H.W. performed data acquisition and analysis. A.G. jointly supervised. N.D.F. wrote and edited the original manuscript. A.G. administrated the project and acquired the funding. All authors critically reviewed and approved the manuscript.

Acknowledgements

This project has received funding from the European Union's Horizon 2020 research and innovation programme, OXYtrain MSCA-ITN, under grant agreement No 722390. This article was supported by TU Graz Open Access Publishing Fund. The authors are grateful to Prof. Kroutil for access to his chemistry facilities and material.

Conflict of Interest

The authors declare no conflict of interest.

Data Availability Statement

The data that support the findings of this study are available in the supplementary material of this article.

Keywords: Biotransformations · Cytochrome P450 · Enzyme catalysis · Natural products · Preparative-scale synthesis

[1] I. Ahuja, R. Kissen, A. M. Bones, *Trends Plant Sci.* **2012**, *17*, 73–90.
[2] M. Dvorakova, P. Landa, *Pharmacol. Res.* **2017**, *124*, 126–145.
[3] B. De Filippis, A. Ammazzalorso, M. Fantacuzzi, L. Giampietro, C. Maccallini, R. Amoroso, *ChemMedChem* **2017**, *12*, 558–570.
[4] B. Akinwumi, K.-A. Bordun, H. Anderson, *Int. J. Mol. Sci.* **2018**, *19*, 792.
[5] R. Pangeni, J. K. Sahni, J. Ali, S. Sharma, S. Baboota, *Expert Opin. Drug Delivery* **2014**, *11*, 1285–1298.
[6] M. H. Keylor, B. S. Matsuura, C. R. J. Stephenson, *Chem. Rev.* **2015**, *115*, 8976–9027.
[7] M. Savio, D. Ferraro, C. Maccario, R. Vaccarone, L. D. Jensen, F. Corana, B. Mannucci, L. Bianchi, Y. Cao, L. A. Stivala, *Sci. Rep.* **2016**, *6*, 19973.

[8] G.-J. Fan, X.-D. Liu, Y.-P. Qian, Y.-J. Shang, X.-Z. Li, F. Dai, J.-G. Fang, X.-L. Jin, B. Zhou, *Bioorg. Med. Chem.* **2009**, *17*, 2360–2365.
[9] Thapa, Pandey, Park, Kyung Sohng, *Molecules* **2019**, *24*, 2571.
[10] Y.-P. Shen, F.-X. Niu, Z.-B. Yan, L. S. Fong, Y.-B. Huang, J.-Z. Liu, *Front. Bioeng. Biotechnol.* **2020**, *8*, 407.
[11] M. Li, K. Schneider, M. Kristensen, I. Borodina, J. Nielsen, *Sci. Rep.* **2016**, *6*, 36827.
[12] Saraswati S. Velu, Noel F. Thomas, Jean-Frederic F. Weber, *Curr. Org. Chem.* **2012**, *16*, 605–662.
[13] G. Likhtenshtein, *Stilbenes*, Wiley, Weinheim, Germany, **2009**.
[14] K. Xiao, H.-J. Zhang, L.-J. Xuan, J. Zhang, Y.-M. Xu, D.-L. Bai, in *Stud. Nat. Prod. Chem.*, Elsevier, Oxford, **2008**, pp. 453–646.
[15] S. S. Hupp, H. E. Swift, *Ind. Eng. Chem. Prod. Res. Dev.* **1979**, *18*, 117–122.
[16] C. Aranda, R. Ullrich, J. Kiebist, K. Scheibner, J. C. del Río, M. Hofrichter, A. T. Martínez, A. Gutiérrez, *Catal. Sci. Technol.* **2018**, *8*, 2394–2401.
[17] A. Rühlmann, D. Antovic, T. J. J. Müller, V. B. Urlacher, *Adv. Synth. Catal.* **2017**, *359*, 984–994.
[18] P. Jeandet, E. Sobarzo-Sánchez, A. S. Silva, C. Clément, S. F. Nabavi, M. Battino, M. Rasekhian, T. Belwal, S. Habtemariam, M. Koffas, S. M. Nabavi, *Biotechnol. Adv.* **2020**, *39*, 107461.
[19] N. D. Fessner, *ChemCatChem* **2019**, *11*, 2226–2242.
[20] Y. Wang, D. Lan, R. Durrani, F. Hollmann, *Curr. Opin. Chem. Biol.* **2017**, *37*, 1–9.
[21] M. T. Lundemo, J. M. Woodley, *Appl. Microbiol. Biotechnol.* **2015**, *99*, 2465–2483.
[22] N. D. Fessner, C. Grimm, M. Srdič, H. Weber, W. Kroutil, U. Schwaneberg, A. Glieder, *ChemCatChem* **2022**, *14*, e202101564.
[23] M. Winkler, M. Geier, S. P. Hanlon, B. Nidetzky, A. Glieder, *Angew. Chem. Int. Ed.* **2018**, *57*, 13406–13423; *Angew. Chem.* **2018**, *130*, 13592–13610.
[24] C. A. Dra˘gan, F. T. Peters, P. Bour, A. E. Schwaninger, S. M. Schaan, I. Neunzig, M. Widjaja, J. Zapp, T. Kraemer, H. H. Maurer, M. Bureik, *Appl. Biochem. Biotechnol.* **2011**, *163*, 965–980.
[25] D. R. Nelson, *Biochim. Biophys. Acta - Proteins Proteom.* **2018**, *1866*, 141–154.
[26] P. Durairaj, J.-S. Hur, H. Yun, *Microb. Cell Fact.* **2016**, *15*, 125.
[27] W. Chen, M.-K. Lee, C. Jefcoate, S.-C. Kim, F. Chen, J.-H. Yu, *Genome Biol. Evol.* **2014**, *6*, 1620–1634.
[28] K. Syed, K. Shale, N. S. Pagadala, J. Tuszynski, *PLoS One* **2014**, *9*, e86683.
[29] V. B. Urlacher, M. Girhard, *Trends Biotechnol.* **2019**, *37*, 882–897.
[30] H. Park, G. Park, W. Jeon, J.-O. Ahn, Y.-H. Yang, K.-Y. Choi, *Biotechnol. Adv.* **2020**, *40*, 107504.
[31] C. C. C. R. de Carvalho, *Microb. Biotechnol.* **2017**, *10*, 250–263.
[32] S. Chakrabarty, Y. Wang, J. C. Perkins, A. R. H. Narayan, *Chem. Soc. Rev.* **2020**, *49*, 8137–8155.
[33] C. K. Prier, B. Kosjek, *Curr. Opin. Chem. Biol.* **2019**, *49*, 105–112.
[34] J. Dong, E. Fernández-Fueyo, F. Hollmann, C. E. Paul, M. Pesic, S. Schmidt, Y. Wang, S. Younes, W. Zhang, *Angew. Chem. Int. Ed.* **2018**, *57*, 9238–9261; *Angew. Chem.* **2018**, *130*, 9380–9404.
[35] T. Pusztahelyi, I. J. Holb, I. Pócsi, *Front. Plant Sci.* **2015**, *6*, 1–23.
[36] N. D. Fessner, D. R. Nelson, A. Glieder, *Appl. Microbiol. Biotechnol.* **2021**, *105*, 6779–6792.
[37] M. Ide, H. Ichinose, H. Wariishi, *Arch. Microbiol.* **2012**, *194*, 243–253.
[38] N. D. Fessner, H. Weber, A. Glieder, *Biochem. Biophys. Res. Commun.* **2022**, *595*, 35–40.
[39] N. D. Fessner, C. Grimm, W. Kroutil, A. Glieder, *Biomol. Eng.* **2021**, *11*, 1708.
[40] R. Kratzer, J. M. Woodley, B. Nidetzky, *Biotechnol. Adv.* **2015**, *33*, 1641–1652.
[41] A. Braun, M. Geier, B. Bühler, A. Schmid, S. Mauersberger, A. Glieder, *Microb. Cell Fact.* **2012**, *11*, 106.
[42] T. Wriessnegger, P. Augustin, M. Engleder, E. Leitner, M. Müller, I. Kaluzna, M. Schürmann, D. Mink, G. Zellnig, H. Schwab, H. Pichler, *Metab. Eng.* **2014**, *24*, 18–29.
[43] H. Ichinose, *Biotechnol. Appl. Biochem.* **2013**, *60*, 71–81.
[44] D. R. Nelson, in *Cytochrome P450 Protoc.* (Eds.: I. R. Philips, E. A. Shephard), Humana Press, New Jersey, **2006**, pp. 1–10.
[45] T. Vogl, L. Gebbie, R. W. Palfreyman, R. Speight, *Appl. Environ. Microbiol.* **2018**, *84*, e02712–17.
[46] L. Näätsaari, B. Mistlberger, C. Ruth, T. Hajek, F. S. Hartner, A. Glieder, *PLoS One* **2012**, *7*, e39720.
[47] J. M. Klenk, B. A. Nebel, J. L. Porter, J. K. Kulig, S. A. Hussain, S. M. Richter, M. Tavanti, N. J. Turner, M. A. Hayes, B. Hauer, S. L. Flitsch, *Biotechnol. J.* **2017**, *12*, 1600520.
[48] J. Wachtmeister, D. Rother, *Curr. Opin. Biotechnol.* **2016**, *42*, 169–177.
[49] T. Vogl, T. Kickenweiz, J. Pitzer, L. Sturmberger, A. Weninger, B. W. Biggs, E.-M. Köhler, A. Baumschlager, J. E. Fischer, P. Hyden, M. Wagner, M. Baumann, N. Borth, M. Geier, P. K. Ajikumar, A. Glieder, *Nat. Commun.* **2018**, *9*, 3589.
[50] X. Cui, Z. Li, C.-Z. Tao, Y. Xu, J. Li, L. Liu, Q.-X. Guo, *Org. Lett.* **2006**, *8*, 2467–2470.
[51] R. B. Chhor, K. A. Singh, B. Nosse, V. K. Tandon, *Synth. Commun.* **2003**, *33*, 2519–2530.
[52] A. Shard, N. Sharma, R. Bharti, S. Dadhwal, R. Kumar, A. K. Sinha, *Angew. Chem.* **2012**, *124*, 12416–12419; *Angew. Chem. Int. Ed.* **2012**, *51*, 12250–12253.
[53] G. Orgován, I. Gonda, B. Noszál, *J. Pharm. Biomed. Anal.* **2017**, *138*, 322–329.
[54] H.-Y. Sun, C.-F. Xiao, Y.-C. Cai, Y. Chen, W. Wei, X.-K. Liu, Z.-L. Lv, Y. Zou, *Chem. Pharm. Bull.* **2010**, *58*, 1492–1496.
[55] M. Deak, H. Falk, *Monatsh. Chem.* **2003**, *134*, 883–888.
[56] M. Guiso, C. Marra, A. Farina, *Tetrahedron Lett.* **2002**, *43*, 597–598.

Manuscript received: November 26, 2021
Revised manuscript received: April 15, 2022
Accepted manuscript online: April 19, 2022